

ON THE INTERFACIAL BEHAVIOR ABOUT THE SHIELD REGION

Andrés Mejía and Hugo Segura *

Group of Thermodynamics. Department of Chemical Engineering, Universidad de Concepción, POB 160-C, Fax : 56-41-247491, Concepción, Chile.

* To whom correspondence should be addressed. Email : hsegura@diq.udec.cl

ABSTRACT

The shield region is a singular range of the Global Phase Diagram, where equations of state based on mean field theories predict a quadruple point for fluid binary mixtures. The quadruple point in question is characterized by three immiscible liquids and a vapor in equilibrium. No experimental system has been found exhibiting such an equilibrium behavior. In this theoretical work we describe the interfacial and wetting behavior of the phases that coexist at the quadruple point by applying the gradient theory to the van der Waals equation of state.

Introduction

In 1968, van Konynenburg and Scott [1, 2] published a seminal work regarding the capability of the van der Waals equation of state (vdW-EOS) to predict fluid phase equilibrium diagrams in binary mixtures. As a result it was found that the vdW model originates five main Types, or classes, that differ essentially on the geometry and connectivity of the predicted critical lines. Mixtures that classify inside a same Type exhibit phase diagrams of equivalent shapes and, consequently, they display similar equilibrium behavior over the whole subcritical range. A remarkable contribution of the work of van Konynenburg and Scott was the development of a map, that they called “Master Diagram” (or Global Phase Diagram, GPD), where the prediction of each Type was bounded in terms of the parameters of the vdW-EOS. Since the work of van Konynenburg and Scott, the GPD approach has been further developed, becoming a powerful tool of analysis both in theoretical and applied thermodynamics. A reduced set of GPDs have been calculated for van der Waals type and theoretically based EOSs [3-11]. These works, restricted mainly to mixtures of molecules of equal size, focus on finding all conceivable phase equilibrium behavior and allow to conclude that EOSs display similar GPDs. Among the most interesting phenomena found are the ability of simple models to predict four-phase equilibria inside the *shield region* [5, 12] and the less known *sword region*. [13]

In order to extend the systematic approach of the GPD to the case of interfacial fluids, several authors [13-24] have characterized some of their regions in terms of the thermal dependence of interface tensions and in terms of wetting transitions. From these works, devoted mainly to two or three phase equilibrium, we have a better understanding of the relation between the interfacial behavior and the topologic Type.

The scope of this work is to fill some gaps regarding the interfacial behavior of mixtures that belong to the shield region (Sh-r) [12]. As pointed out before, the Sh-r is characterized by a quadruple point (QP) of equilibrium where three immiscible liquids and a gas coexist. Although no experimental binary mixture has been found exhibiting such an equilibrium behavior, a quadruple point of fluid phases is itself interesting, since it is possible to expect a condition high interfacial activity. In our analysis we applied the square gradient theory to vdW binary mixtures of molecules of equal size [14].

Theory

The Shield Region

Figure 1 depicts the Sh-r predicted by the vdW-EOS considering molecules of equal size. The coordinates of this Figure are related to the parameters of the EOS according to the following definitions [1, 2] :

$$\xi = \frac{b_2 - b_1}{b_2 + b_1} \quad ; \quad \zeta = \frac{a_2/b_2^2 - a_1/b_1^2}{a_2/b_2^2 + a_1/b_1^2} \quad ; \quad \lambda = \frac{a_2/b_2^2 - 2a_{12}/b_{12}^2 + a_1/b_1^2}{a_2/b_2^2 + a_1/b_1^2} \quad (1)$$

In Eq.1, a_i is the cohesion parameter and b_i is the covolume that, for pure vdW fluids, depend on critical temperature T_c and pressure P_c according to :

$$a_i = \frac{27 (RT_{ci})^2}{64 P_{ci}} \quad ; \quad b_i = \frac{1 RT_{ci}}{8 P_{ci}} \quad (2)$$

where R is the gas constant. In addition, the cross parameters a_{ij} , b_{ij} of Eq. 1 are given by :

$$a_{12} = \sqrt{a_1 a_2} (1 - k_{12}) \quad ; \quad b_{12} = \frac{b_1 + b_2}{2} \quad (3)$$

In Eq. 3, k_{12} is the interaction parameter that accounts for the magnitude and sign of deviation of the mixture from ideal behavior.

As shown in Figure 1, the Sh-r for mixtures of molecules of equal size ($\xi = 0$) is an almost triangular symmetric region where three tricritical boundaries, a critical pressure step point (CPSP) boundary and a limiting azeotropic-heteroazeotropic boundary (III-A-H line) converge. A CPSP transition bounds the behavior of multiple stationary points in pressure along a critical line in a P-T projection. In addition, the III-A-H line masks the azeotropic behavior inside a range of immiscibility. Finally, a tricritical transition breaks the continuity of a critical line in a critical end point (CEP). Due to all these transitional mechanisms, the systems that may be found inside the Sh-r are hybrids of Types II and III that may present stationary pressure points and/or azeotropic behavior.

Figure 2.a depicts a particular P-T projection that may be found inside the Sh-r [$\zeta = 0.04$, $\lambda = 0.46$]. Due to the previously mentioned transitional mechanisms, the general trend and connectivity of the main critical lines vary as the coordinates ζ , λ change. However, every system drawn from the region in question exhibits QPs, as the shown in Figures 2, with the following similarities

- the QP appears below the critical temperature of the constituents of the mixture, connecting a low temperature three-phase line with three high temperature three-phase lines.
- the pressure of the QP is larger than the vapor pressure of pure components.
- at the QP, three phases have liquid-type densities and the remaining phase has gas-type density.

Figures 2.c to 2.d depict the phase diagrams that appear in the vicinity of the QP. It should be pointed out that the shapes of these diagrams are characteristic for every mixture inside the Sh-r. In the quoted Figures it is possible to recognize a liquid phase α rich in component 2 and a second liquid phase β rich in component 1. The concentrations of the gas phase G are bounded by the concentrations of α and β . In addition, starting from the temperature of the QP, a third liquid phase γ appears and it induces a bifurcation of the low temperature three-phase line. The liquid γ is characterized by mid-range concentrations and, depending on the coordinates of the GPD, it is able to form azeotropes.

The boundaries of the Sh-r may be calculated considering that two phases of the QP collapse in an ordinary critical point (the phases that become critical are indicated in Figure 1). In addition, every vertex of the Sh-r corresponds to a condition where three phases of the QP collapse in a tricritical point.

In this work, we analyze the interfacial properties of the set of three phase lines for a system with fixed ζ , λ coordinates. Then we consider the interfacial properties of the QP for displacements in ζ and in λ , in order to assess the influence of the components of the mixture and the synergy between components, respectively.

The square gradient theory for planar interfaces

According to the gradient theory (GT) the interfacial tension (σ) between two bulk phases at equilibrium (α , β) is given by [23]

$$\sigma = \sqrt{2} \int_{\rho_s^\alpha}^{\rho_s^\beta} \sqrt{\left(a_0 - \sum_{i=1}^{n_c} \rho_i \mu_i^0 + P^0 \right) \sum_{i,j=1}^{n_c} c_{ij} \frac{d\rho_i}{d\rho_s} \frac{d\rho_j}{d\rho_s}} d\rho_s \quad (4)$$

In this expression, $\rho_{i,j}$ are the concentrations of species i and j , ρ_s is a reference concentration (for component i or j) whose behavior should be monotonically defined along the integral path. P^0 is the bulk equilibrium pressure, n_c stands for the number of components, a_0 is the density of the Helmholtz energy of the homogeneous system, μ_i^0 is the chemical potential of component i at equilibrium. Both a_0 and μ_i^0 can be determined directly from any EOS [24]. c_{ij} is the cross influence parameter that was considered constant. In the present work, c_{ij} is calculated from the following expressions [23, 24]

$$\frac{c_{ii}}{a_{ii} b_{ii}^{2/3}} = \left(\frac{3}{2\pi N_{av}} \right)^{2/3} \quad ; \quad c_{ij} = \sqrt{c_{ii} c_{jj}} \quad (5)$$

where N_{av} is the Avogadro constant. In Eq. 4, ρ_i and ρ_j are related by a set of partial differential equations (PDE) that describe the equilibrium condition for the interfacial fluid. However, Eqs. 5 allow to simplify the PDE problem to the following set of algebraic equations [23]

$$\sqrt{c_{ss}} [\mu_k(\rho) - \mu_k^0] = \sqrt{c_{kk}} [\mu_s(\rho) - \mu_s^0] \quad k = 1, 2, \dots, s-1, s+1, \dots, n_c \quad (6)$$

Equation 6 allows to quantify the population of species at the interface, together with the surface activity which is characterized by the condition $(d\rho_i/d\rho_j) = 0$ [23]. Physically significant solutions of Eqs. 6 should be bounded by the hard core limit of the EOS (in this case the covolume) since at that limit $\mu_i \rightarrow -\infty$. The numerical procedure that allows to calculate σ from Eqs. 4 and 6 was described in detail in a previous work [24].

Wetting transitions at fluid interfaces

π phases in equilibrium may be contacted by a maximum of $[\frac{1}{2}(\pi - 1)\pi]$ interfaces, each one of which is characterized by an specific value of σ . For the case of three phases in equilibrium (α, β, γ) the interfacial tensions ($\sigma_{\alpha\beta}, \sigma_{\alpha\gamma}, \sigma_{\beta\gamma}$) are interrelated by [14]:

$$\sigma_{\alpha\beta} < \sigma_{\alpha\gamma} + \sigma_{\beta\gamma} \quad \text{partial wetting or } \textit{Neumman inequality} \quad (7.a)$$

$$\sigma_{\alpha\beta} = \sigma_{\alpha\gamma} + \sigma_{\beta\gamma} \quad \text{total wetting or } \textit{Antonow rule} \quad (7.b)$$

the wetting condition is invariant to the cyclic permutation of the subindices α, β, γ . As written, Eqs. 7 describe the partial and total wetting of the γ phase on the $\alpha\beta$ interface. The transition from partial to total wetting (or vice versa) is called *wetting transition* [14]. For the case of $\pi > 3$, no general rule exists to establish the mathematical condition of a wetting transition. Intuitively, it is possible to infer that a basic condition for a wetting transition is that at the least every set of $(\pi - 1)$ phases should be at the wetting transition. Following this argument, we can expect that a wetting transition at the QP ($\pi = 4$) requires a wetting transition condition for every set of three phases that we could select from the QP. Following such an hypothesis the wetting transitions of a QP may be analyzed using Eqs. 7.

Results and Discussion

Interface behavior at fixed ζ, λ coordinate

The objective of this section is to analyze the $\rho - \rho$ and $\sigma - T$ projections for a specific QP inside the Sh-r, and to illustrate the connectivity of interfacial properties at the QP. The GPD coordinates, critical properties and interaction parameter of the mixture are indicated in Table I. Figures 2 illustrate the critical P-T projection and the phase diagrams for the system in question. The thermal evolution of the $\rho - \rho$ projections for each three phase line that meets the QP is shown in Figures 3. From these figures we can conclude that the Sh-r exhibits dominant surface activity, as follows from the condition $(dp_i/dp_j) = 0$. Inspection of Figures 3 reveals that the $\rho - \rho$ projections of every three phase line converge to a single trajectory at the QP, whose $\rho - \rho$ projection is shown in Figure 4. Figures 5 and 6 show the $\sigma - T$ projections for the complete set of three phase lines connecting at the QP. The interfacial behavior of mixture under analysis is summarized in Tables II and III. From these results, we can conclude that the interfacial tensions along the three-phase lines exhibit the usual trend that can be expected for heteroazeotropes at subcritical and critical conditions, as we described in a previous work [24].

Focusing our attention on the QP, we can observe that the interfacial tensions of the low temperature three phase line connect the interfacial tensions of the high temperature three phase lines for the $\alpha\beta, \alpha G$ and βG interfaces. It is clear also that the temperature slope of these interfacial tensions change at the QP. In addition, due to the generation of the γ phase,

additional interfacial tensions related to the γ interface appear at $T \geq T_{QP}$. In fact The QP is characterized by six interfacial tensions of different orders of magnitude.

Interface behavior for the QP along the λ coordinate ($\zeta = 0.0404$).

The objective of this section is to assess the impact of the λ coordinate on the interface behavior. From Eqs. 1, it follows that λ displacements are related to variations of k_{12} . A constant ζ value implies that the critical properties of mixture do not vary as λ changes. Consequently, this analysis reflects the influence of the synergy of the mixture on the interfacial properties of the QP.

Figure 7 depicts the evolution of $\rho - \rho$ projection as λ increases. Minor variations could be observed, allowing to deduce that the surface activity of the interface does not vary significantly with λ .

Figures 8 illustrate the evolution of the six interfacial tensions of the QP. We can observe that, as λ increases, four interfacial tensions increase ($\sigma_{\alpha G}$, $\sigma_{\alpha\gamma}$, $\sigma_{\alpha\beta}$, $\sigma_{\beta\gamma}$) and two decrease ($\sigma_{\beta G}$, $\sigma_{\gamma G}$). In addition, these Figures show that interfacial behavior is in agreement with the critical collapse of the γG and the $\alpha\gamma$ phases at the upper and lower limits of the Sh-r (see Figure 1). General results have been summarized in Table IV.

Similar results can be found for every $\zeta \in (0 ; 0.0507]$. As a consequence of the symmetry of the GPD, the range $\zeta \in [-0.0507 ; 0)$ exhibits the same patterns described before. Finally, analyzing the curves $\sigma(\lambda)$ and using the Eqs. 7 we can conclude that, for the analyzed ranges, no wetting transitions are observed at the QP.

Interface behavior for the QP along to ζ coordinate ($\lambda = 0.4550$)

The objective of this section is to analyze the $\rho - \rho$ and $\sigma - \zeta$ projections of a QP at a fixed λ value. Such an incursion reflects the influence of the critical properties of the constituents of a mixture. Figure 9 shows the $\rho - \rho$ projections for different ζ values. From this Figure it is possible to conclude that variations on the ζ coordinate affects strongly the surface activity. Such a behavior follows from the fact that ζ variations change the c_{ij} values. In Figure 9 we can also see that, as ζ decreases from 0.0507 to 0, the solutions of Eqs. 6 tend to the limit $\mu_i \rightarrow -\infty$. Specifically, at $\zeta = 0$, the $\rho - \rho$ projection becomes discontinuous. Such a discontinuity follows from the fact that the mixture is composed by equivalent molecules with large synergy. Figure 10 shows the $\rho - \rho$ projections for the full ζ range, $\zeta \in [-0.0507 ; 0.0507]$.

Figures 11 show the dependence of σ on ζ . As was shown in Figures 4 and 8, the QP is characterized by high and low interface tensions. In Figure 11 we can observe that, as ζ increases, five interfacial tensions increase ($\sigma_{\alpha G}$, $\sigma_{\alpha\gamma}$, $\sigma_{\alpha\beta}$, $\sigma_{\beta\gamma}$, $\sigma_{\beta G}$) and one decreases ($\sigma_{\gamma G}$). It is also observed that the trend of interfacial tensions agree with the phases of the QP that become critical at the left and right hand side limits of the Sh-r. General results have been summarized in Table IV. Finally, the analysis of the curves $\sigma(\zeta)$ reveals that no wetting transitions are observed along the ζ coordinate.

Concluding Remarks

In this work we have analyzed interface properties and wetting transitions for mixtures of molecules of equal size inside the shield region. Special attention has been given to the properties of the quadruple point. Calculations have been based on the GT applied the vdW-EOS. The main advantage of such an approach is that the same EOS is used to predict phase equilibrium as well as interfacial properties. According to results, the shield region is characterized by qualitatively similar $\rho - \rho$ projections and strong surface activity. In addition, $\rho - \rho$ projections are very sensitive to changes in the ζ coordinate, due to variation of the influence parameter c_{ij} , and less sensitive to the λ coordinate. It follows then that the interfacial properties of the shield region exhibit strong dependence on the mixture and weak dependence on its synergy

The QP of the shield region are characterized by six interfacial tensions of different orders of magnitude. Our results show no wetting transitions for the QP of molecules of equal sizes.

Acknowledgments

This work was financed by FONDECYT, Santiago, Chile (Project 2010100).

References

- [1] van Konynenburg, P. Critical Lines and Phase Equilibria in Binary van der Waals Mixtures. Ph.D. Thesis, **1968**, University of California.
- [2] van Konynenburg, P. ; Scott, R. *Phil. Trans. Royal Society (London)* , **1980**, 298 A, 495.
- [3] D. Furman, S. Dattagupta, and R. B. Griffiths, *Phys. Rev. B*, **1977**, 15, 441.
- [4] Boshkov, L. Z. and Mazur, V. A. *Russ. J. Phys. Chem.* **1986**, 60, 16.
- [5] I.-C. Wei and R. L. Scott, *J. Stat. Phys.*, **1988**, 52, 1315.
- [6] P. H. E. Meijer, O. L. Pegg, J. Aronson, M. Keskin, *Fluid Phase Equil.*, **1990**, 58, 65.
- [7] L. Z. Boshkov and L. V. Yelash, *Fluid Phase Equil.*, **1997**, 141, 105.
- [8] L. Z. Boshkov and L. V. Yelash, *Doklady Akademii Nauk*, **1995**, 341, 61.
- [9] U. K. Deiters and I. L. Pegg, *J. Chem. Phys.*, **1989**, 90, 6632.
- [10] T. Kraska and U. K. Deiters, *J. Chem. Phys.*, **1991**, 96, 539.
- [11] T. Kraska. *Ber. Bunsenges. Phys. Chem.* **1996**, 100, 1318.
- [12] D. Furman and R. B. Griffiths, *Phys. Rev. A*, **1978**, 17, 1139.
- [13] U. K. Deiters, L. Z. Boshkov, L. V. Yelash, and V. A. Mazur, *Doklady Akademii Nauk*, **1998**, 359, 343.
- [14] Rowlinson, J. S. ; Widom, B. **1982**, “*Molecular Theory of Capillarity*,” Oxford University Press, Oxford.
- [15] Sullivan, D. E. *J. Chem. Phys.*, **1982**, 77, 2632
- [16] Costas, M. E. ; Vera, C. ; Robledo, *Phys. Rev. Lett.* **1983**, 51, 2394.
- [17] Cornelisse, P. M. W. The Gradient Theory Applied, Simultaneous Modelling of Interfacial Tension and Phase Behaviour, Ph.D. Thesis, **1997**, Delft University.
- [18] McLure, I.A.; Whitfield, R.; Bowers, J. *J. Colloid Interface Sci.* **1998**, 203, 31

- [19] Pérez C. ; Roquero, P. ; Talanquer, V. *J. Chem. Phys.*, **1994**, *100*, 5913
- [20] Telo da Gama, M. M. ; Evans, R. *Molec. Phys.*, **1983**, *48*, 229
- [21] Telo da Gama, M. M. ; Evans, R. *Molec. Phys.*, **1983**, *48*, 251
- [22] Tarazona, P. ; Telo da Gama, M. M. ; Evans, R. *Molec. Phys.*, **1983**, *49*, 283
- [23] Carey, B.S. The Gradient Theory of Fluid Interfaces, Ph.D. Thesis, **1979**, University of Minnesota.
- [24] Mejía A., Segura H. Interfacial Behavior in Systems Type IV. Paper to present at the Fifteenth Symposium on Thermophysical Properties, June 22 - 27, 2003, Boulder, Colorado, USA

Table I. GDP coordinates, critical properties and interaction parameter for the mixture

ζ	λ	T_{c2} / T_{c1}	P_{c2} / P_{c1}	k_{12}
0.040400	0.455000	1.084109	1.084109	0.454556

Table II. Interfacial tension behavior along to three phase equilibria

[$\alpha\beta\text{GE}$]		
<i>Temperature Range</i>	<i>Phase Equilibria Type</i>	<i>Interfacial tension behavior</i>
$T < T_{\text{QP}}$	<i>subcritical equilibria</i> $\alpha\text{G}, \beta\text{G}$	$\sigma_{\alpha\text{G}} \neq \sigma_{\beta\text{G}} \neq \sigma_{\alpha\beta} \neq 0$ σ decreases as T increases
	$\alpha\beta$	σ decreases and increases as T increases
$T = T_{\text{QP}}$	<i>subcritical equilibria</i> $\alpha\text{G}, \beta\text{G}, \alpha\beta$	$\sigma_{\alpha\text{G}} \neq \sigma_{\beta\text{G}} \neq \sigma_{\alpha\beta} \neq 0$
[$\alpha\beta\gamma\text{E}$]		
<i>Temperature Range</i>	<i>Phase Equilibria Type</i>	<i>Interfacial tension behavior</i>
$T = T_{\text{QP}}$	<i>subcritical equilibria</i> $\alpha\beta, \alpha\gamma, \beta\gamma$	$\sigma_{\alpha\beta} \neq \sigma_{\alpha\gamma} \neq \sigma_{\beta\gamma} \neq 0$
	<i>subcritical equilibria</i> $\alpha\gamma, \beta\gamma$	$\sigma_{\alpha\beta} \neq \sigma_{\alpha\gamma} \neq \sigma_{\beta\gamma} \neq 0$ σ decreases as T increases
$T_{\text{QP}} < T < T_{\text{UCEP1}}$	$\alpha\beta$	σ increases and decreases as T increases
	<i>subcritical equilibria</i> $\alpha\beta, \alpha\gamma$	$\sigma_{\alpha\beta} \neq \sigma_{\alpha\gamma} \neq 0$
$T = T_{\text{UCEP1}}$	<i>critical equilibria</i> $\beta\gamma$	$\sigma_{\beta\gamma} = 0$
[$\alpha\gamma\text{GE}$]		
<i>Temperature Range</i>	<i>Phase Equilibria Type</i>	<i>Interfacial tension behavior</i>
$T = T_{\text{QP}}$	<i>subcritical equilibria</i> $\alpha\gamma, \alpha\text{G}, \gamma\text{G}$	$\sigma_{\alpha\gamma} \neq \sigma_{\alpha\text{G}} \neq \sigma_{\gamma\text{G}} \neq 0$
	<i>subcritical equilibria</i> $\alpha\text{G}, \gamma\text{G}$	$\sigma_{\alpha\gamma} \neq \sigma_{\alpha\text{G}} \neq \sigma_{\gamma\text{G}} \neq 0$ σ increases as T increases
$T_{\text{QP}} < T < T_{\text{UCEP2}}$	$\alpha\gamma$	σ decreases as T increases
	<i>subcritical equilibria</i> $\alpha\text{G}, \gamma\text{G}$	$\sigma_{\alpha\text{G}} \neq \sigma_{\gamma\text{G}} \neq 0$
$T = T_{\text{UCEP2}}$	<i>critical equilibria</i> $\alpha\gamma$	$\sigma_{\alpha\gamma} = 0$
[$\beta\gamma\text{GE}$]		
<i>Temperature Range</i>	<i>Phase Equilibria Type</i>	<i>Interfacial tension behavior</i>
$T = T_{\text{QP}}$	<i>subcritical equilibria</i> $\gamma\beta, \gamma\text{G}, \beta\text{G}$	$\sigma_{\gamma\beta} \neq \sigma_{\gamma\text{G}} \neq \sigma_{\beta\text{G}} \neq 0$
	<i>subcritical equilibria</i> $\gamma\beta, \gamma\text{G}, \beta\text{G}$	$\sigma_{\alpha\text{G}} \neq \sigma_{\beta\text{G}} \neq \sigma_{\alpha\beta} \neq 0$ σ decreases as T increases
$T_{\text{QP}} < T < T_{\text{UCEP3}}$	$\beta\text{G} = \gamma\text{G}$	$\sigma_{\beta\text{G}} = \sigma_{\gamma\text{G}} \neq 0$
	<i>critical equilibria</i> $\beta\gamma$	$\sigma_{\beta\gamma} = 0$

Table III. Wetting behavior along to three phase equilibria

[$\alpha\beta\text{GE}$]		
<i>Temperature Range</i>	<i>Wetting behavior</i>	<i>Transition Temperature</i>
$T \leq T_{\text{QP}}$	$\sigma_{\alpha\beta} < \sigma_{\alpha\text{G}} + \sigma_{\beta\text{G}}$ $\sigma_{\alpha\text{G}} < \sigma_{\alpha\beta} + \sigma_{\beta\text{G}}$ $\sigma_{\beta\text{G}} < \sigma_{\alpha\beta} + \sigma_{\alpha\text{G}}$	<i>No Wetting Transition</i>
[$\alpha\beta\gamma\text{E}$]		
<i>Temperature Range</i>	<i>Wetting behavior</i>	<i>Transition Temperature</i>
$T_{\text{Q}} < T < T_{\text{UCEP1}}$	$\sigma_{\alpha\gamma} < \sigma_{\alpha\beta} + \sigma_{\gamma\beta}$ $\sigma_{\gamma\beta} < \sigma_{\alpha\gamma} + \sigma_{\alpha\beta}$	<i>No Wetting Transition</i>
$T_{\text{QP}} < T < T_{\text{w}}$	$\sigma_{\alpha\beta} < \sigma_{\alpha\gamma} + \sigma_{\gamma\beta}$	<i>No Wetting Transition</i>
$T = T_{\text{w}}$	$\sigma_{\alpha\beta} = \sigma_{\alpha\gamma} + \sigma_{\gamma\beta}$	$T_{\text{w}} = 0.79605$
$T_{\text{w}} < T < T_{\text{UCEP1}}$	$\sigma_{\alpha\beta} > \sigma_{\alpha\gamma} + \sigma_{\gamma\beta}$	<i>No Wetting Transition</i>
[$\alpha\gamma\text{GE}$]		
<i>Temperature Range</i>	<i>Wetting behavior</i>	<i>Transition Temperature</i>
$T_{\text{QP}} < T < T_{\text{UCEP2}}$	$\sigma_{\alpha\gamma} < \sigma_{\alpha\text{G}} + \sigma_{\gamma\text{G}}$ $\sigma_{\gamma\text{G}} < \sigma_{\alpha\gamma} + \sigma_{\alpha\text{G}}$	<i>No Wetting Transition</i>
$T_{\text{QP}} < T < T_{\text{w}}$	$\sigma_{\alpha\text{G}} < \sigma_{\alpha\gamma} + \sigma_{\gamma\text{G}}$	<i>No Wetting Transition</i>
$T = T_{\text{w}}$	$\sigma_{\alpha\text{G}} = \sigma_{\alpha\gamma} + \sigma_{\gamma\text{G}}$	$T_{\text{w}} = 0.8007$
$T_{\text{w}} < T < T_{\text{UCEP2}}$	$\sigma_{\alpha\text{G}} > \sigma_{\alpha\gamma} + \sigma_{\gamma\text{G}}$	<i>No Wetting Transition</i>
[$\beta\gamma\text{GE}$]		
<i>Temperature Range</i>	<i>Wetting behavior</i>	<i>Transition Temperature</i>
$T_{\text{QP}} < T < T_{\text{UCEP3}}$	$\sigma_{\alpha\beta} < \sigma_{\alpha\text{G}} + \sigma_{\beta\text{G}}$ $\sigma_{\alpha\text{G}} < \sigma_{\alpha\beta} + \sigma_{\beta\text{G}}$ $\sigma_{\beta\text{G}} < \sigma_{\alpha\beta} + \sigma_{\alpha\text{G}}$	<i>No Wetting Transition</i>

Table IV. Interfacial behavior at Shield Region limits

<i>Shield Region limits</i>	<i>Phase Equilibria Type</i>	<i>Interfacial tension behavior</i>
γG	<i>subcritical equilibria</i>	$\sigma_{\beta G} \neq 0; \sigma_{\alpha G} = \sigma_{\alpha\gamma} \neq 0; \sigma_{\beta\gamma} = \sigma_{\beta G} \neq 0$
	$\alpha G, \alpha\beta, \alpha\gamma, \beta G, \beta\gamma$	
$\beta\gamma$	<i>critical equilibria</i>	$\sigma_{\gamma G} = 0$
	γG	
$\alpha\gamma$	<i>subcritical equilibria</i>	$\sigma_{\alpha G} \neq 0; \sigma_{\alpha\beta} = \sigma_{\alpha\gamma} \neq 0; \sigma_{\gamma G} = \sigma_{\beta G} \neq 0$
	$\alpha G, \alpha\beta, \alpha\gamma, \beta G, \gamma G$	
$\alpha\gamma$	<i>critical equilibria</i>	$\sigma_{\beta\gamma} = 0$
	$\beta\gamma$	
$\alpha\gamma$	<i>subcritical equilibria</i>	$\sigma_{\beta G} \neq 0; \sigma_{\alpha\beta} = \sigma_{\beta\gamma} \neq 0; \sigma_{\gamma G} = \sigma_{\alpha G} \neq 0$
	$\alpha G, \alpha\beta, \beta G, \beta\gamma, \gamma G$	
$\alpha\gamma$	<i>critical equilibria</i>	$\sigma_{\alpha\gamma} = 0$
	$\alpha\gamma$	

Figure Captions

- [1] Shield region for equal size molecules calculated from vdW-EOS. α , β , γ immiscible liquids phase, and G gas phase. (—) Tricritical line, (•••) Shield boundary, (—•—) Critical pressure step point line, (— — —) III-A-H
- [2.a] Pressure – Temperature diagram for mixture with QP at $\zeta = 0.0404$, $\lambda = 0.4550$. (—) critical line, (•••) vapor pressure, (—•—) $\alpha\beta\text{GE}$, $\beta\gamma\text{GE}$, $\alpha\gamma\text{GE}$ $\alpha\beta\gamma\text{E}$, (○) QP, (●) UCEPs
- [2.b] Connectivity details around QP in Fig. 2.a
- [2.c] Equilibria diagram for a pre-QP. (○•••○) polyphasic line
- [2.d] Equilibria diagram for a QP. (○•••○) polyphasic line
- [2.e] Equilibria diagram a post-QP. (○•••○) polyphasic line: ① $\beta\gamma\text{G}$, ② $\alpha\gamma\text{G}$, ③ $\alpha\beta\gamma$
- [3] Thermal evolution of interfacial concentrations for the each three phase equilibria. (●) α bulk phase, (○) β bulk phase, (■) γ bulk phase, (□) G bulk phase
- [4] Interfacial concentrations at QP. (●) α bulk phase, (○) β bulk phase, (■) γ bulk phase, (□) G bulk phase
- [5] Thermal evolution of interfacial tension around QP. Zone of high interfacial tension. (—) $\sigma_{\alpha\text{G}}$, (- - -) $\sigma_{\alpha\beta}$, (•••) $\sigma_{\alpha\gamma}$, (●) σ at QP.
- [6] Thermal evolution of interfacial tension around QP. Zone of low interfacial tension. (—•—) $\sigma_{\beta\gamma}$, (-••-) $\sigma_{\beta\text{G}}$, (— —) $\sigma_{\gamma\text{G}}$, (●) σ at QP
- [7] Variation of interfacial concentrations with λ at $\zeta = 0.0404$. (●) α bulk phase, (○) β bulk phase, (■) γ bulk phase, (□) G bulk phase
- [8] High and low zones for the evolution of interfacial tension as a function of λ at $\zeta = 0.0404$. (—) $\sigma_{\alpha\text{G}}$, (- - -) $\sigma_{\alpha\beta}$, (•••) $\sigma_{\alpha\gamma}$, (—•—) $\sigma_{\beta\gamma}$, (-••-) $\sigma_{\beta\text{G}}$, (— —) $\sigma_{\gamma\text{G}}$
- [9] Variation of interfacial concentrations with ζ at $\lambda = 0.4550$. (●) α bulk phase, (○) β bulk phase, (■) γ bulk phase, (□) G bulk phase
- [10] Variation of interfacial concentrations for all ζ range at $\lambda = 0.4550$. (- - -) $\zeta \in [-0.0507 ; 0)$, (—) $\zeta \in (0 ; 0.0507]$

[11] High and low zones for the evolution of interfacial tension as a function of ζ at $\lambda = 0.4550$. (—) $\sigma_{\alpha G}$, (- - -) $\sigma_{\alpha\beta}$, (•••) $\sigma_{\alpha\gamma}$, (-•-) $\sigma_{\beta\gamma}$, (-••-) $\sigma_{\beta G}$, (— —) $\sigma_{\gamma G}$

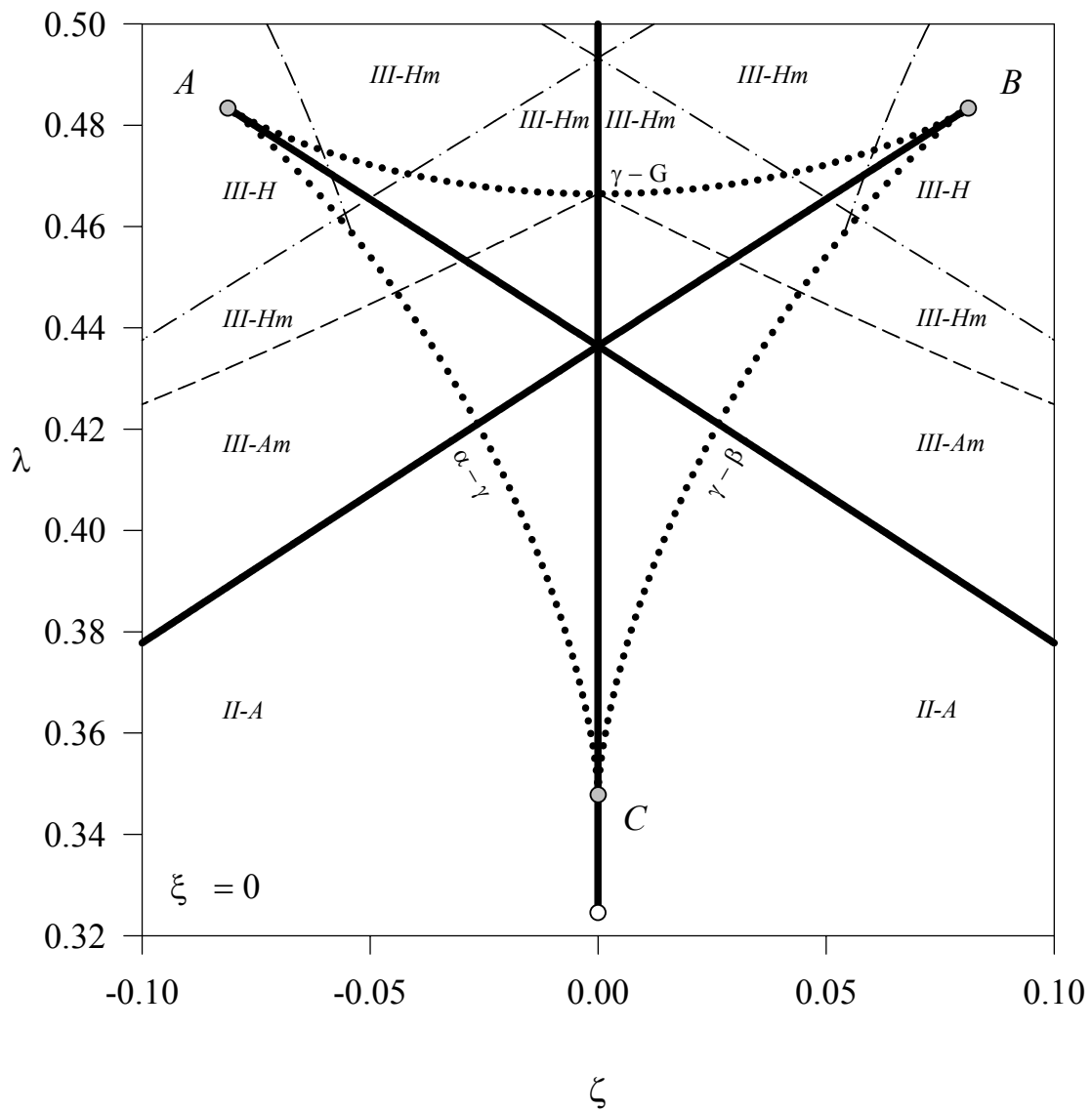


Figure 1

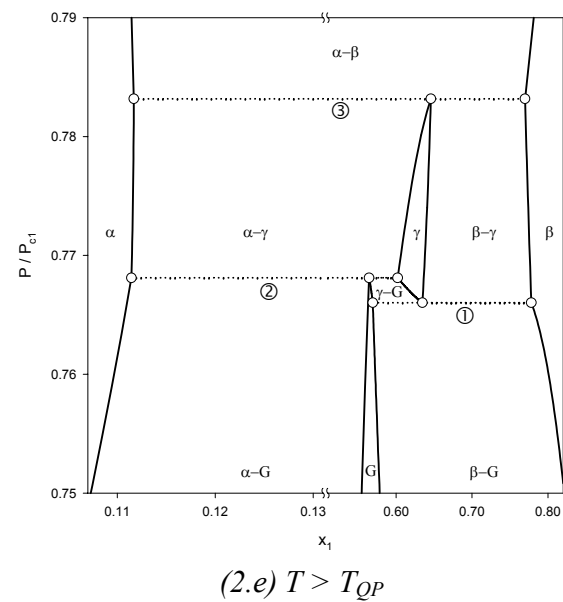
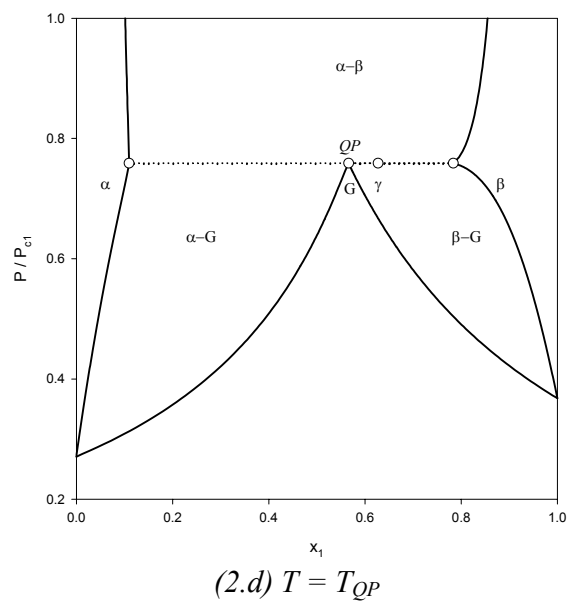
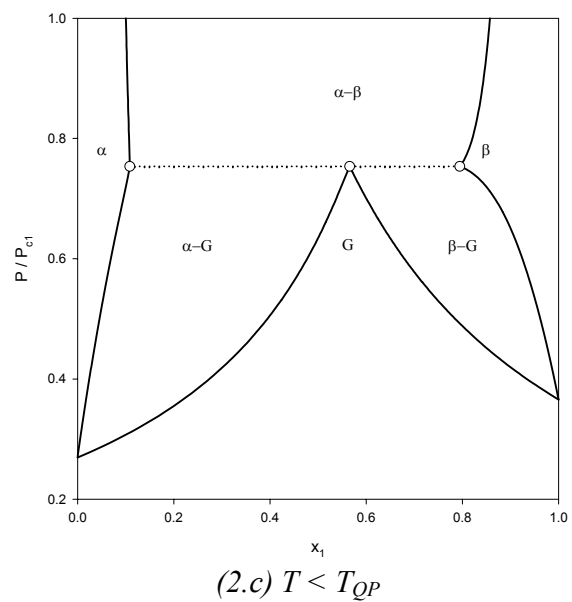
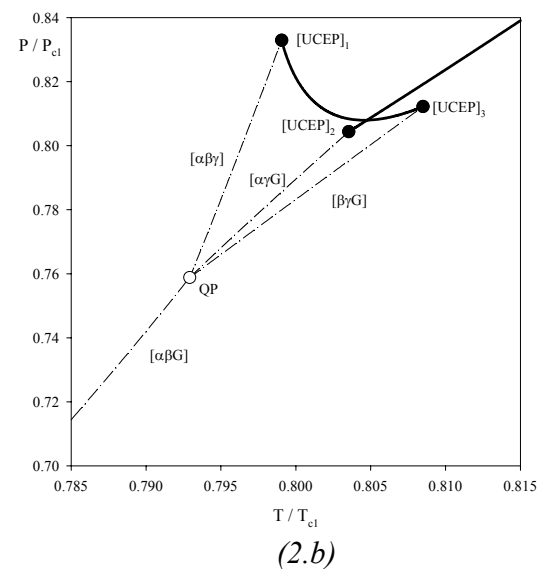
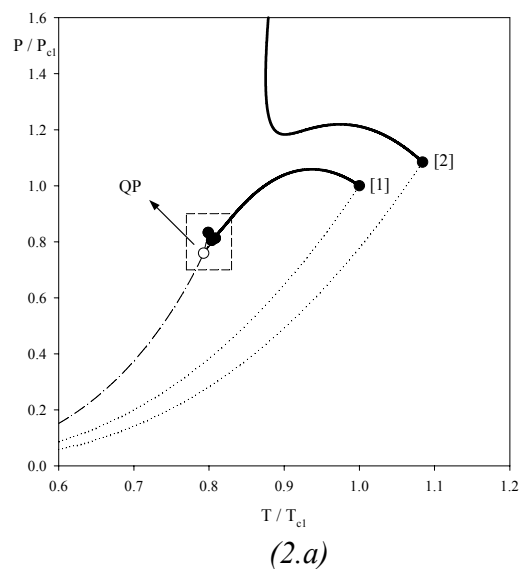


Figure 2

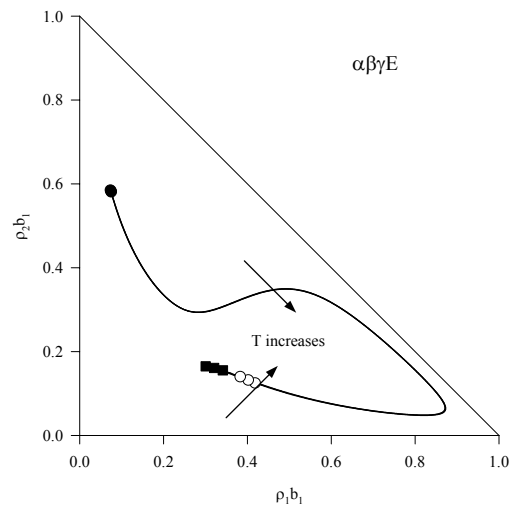
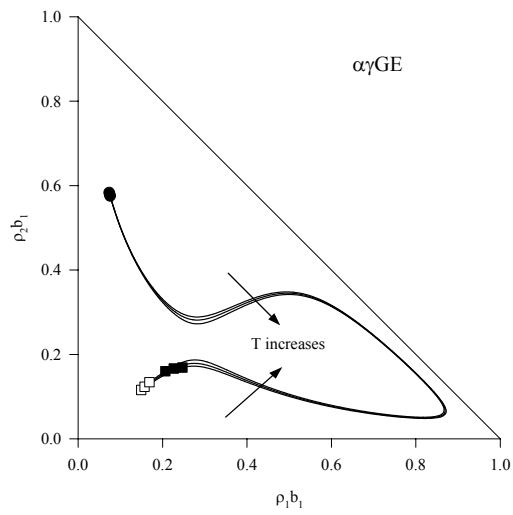
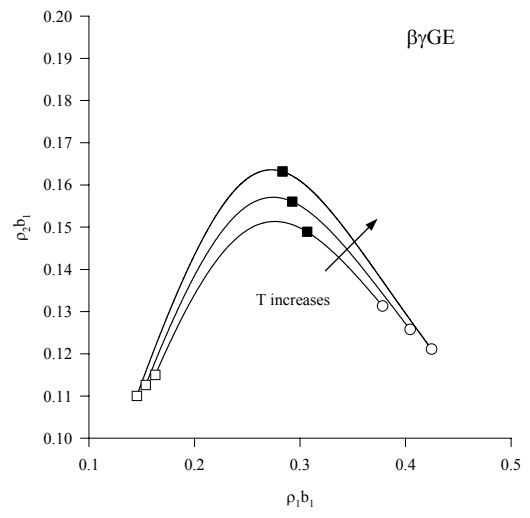
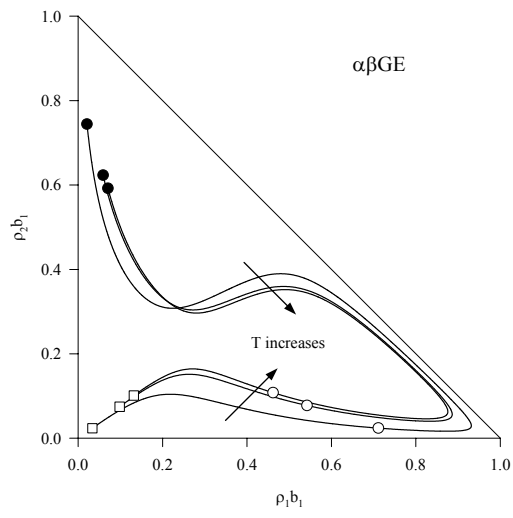


Figure 3

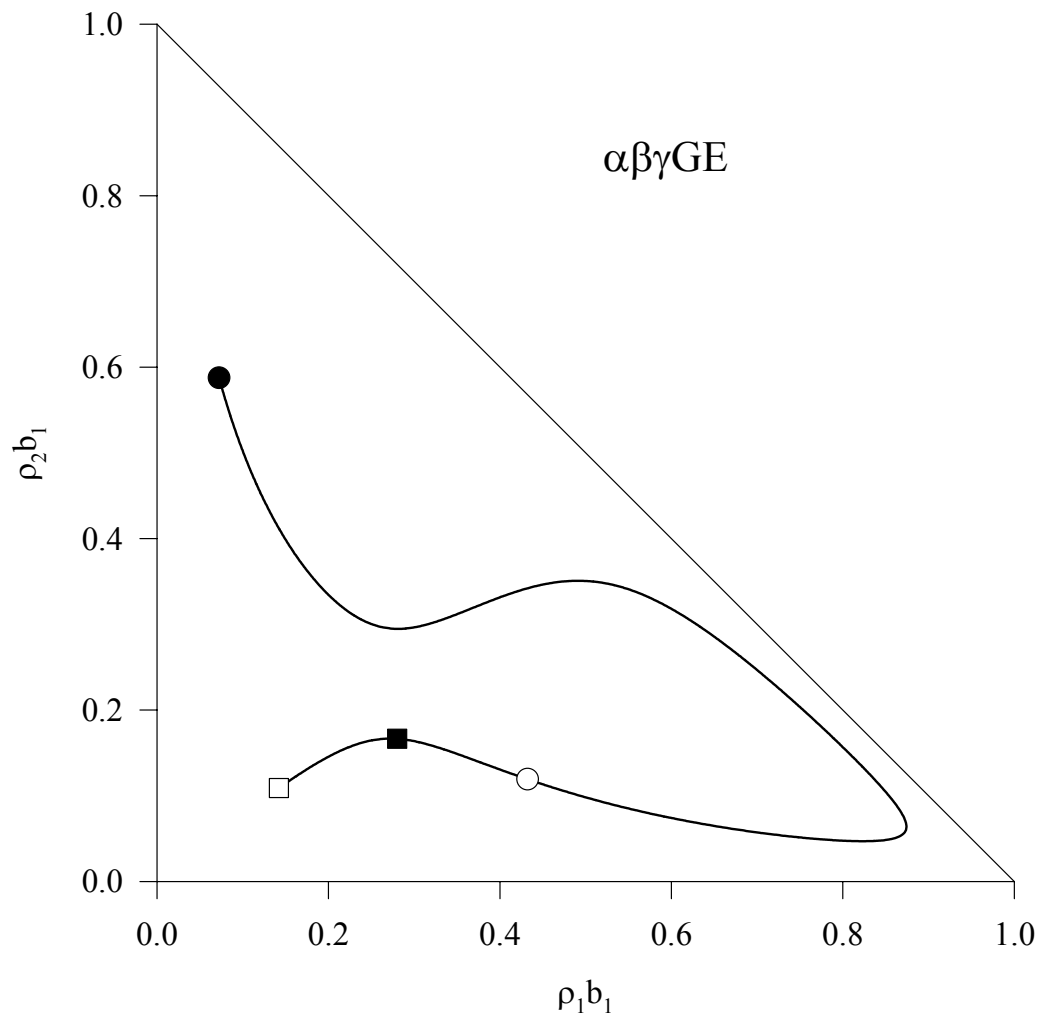


Figure 4

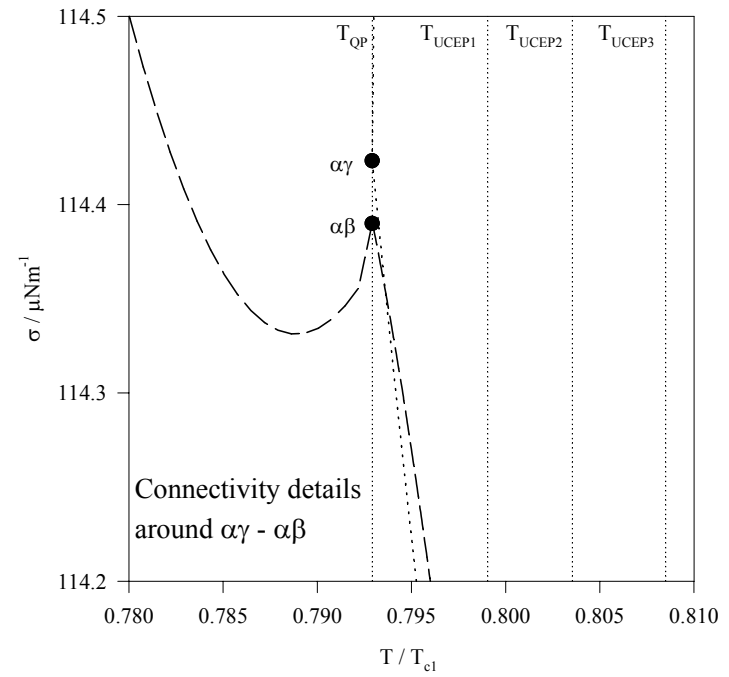
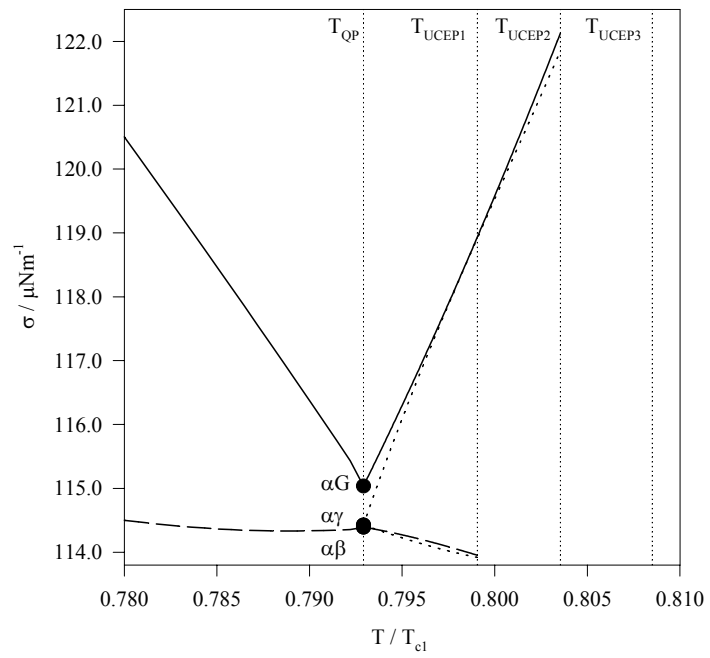


Figure 5

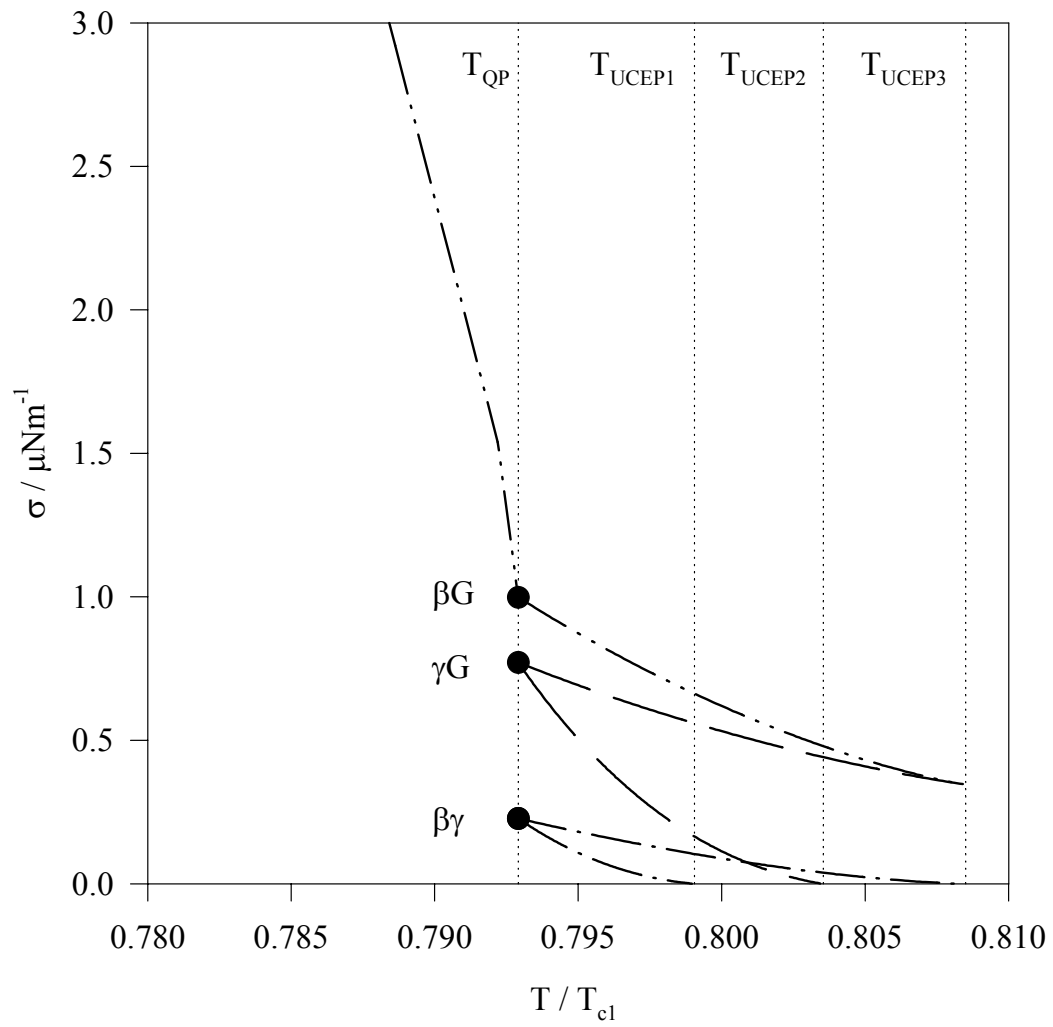


Figure 6

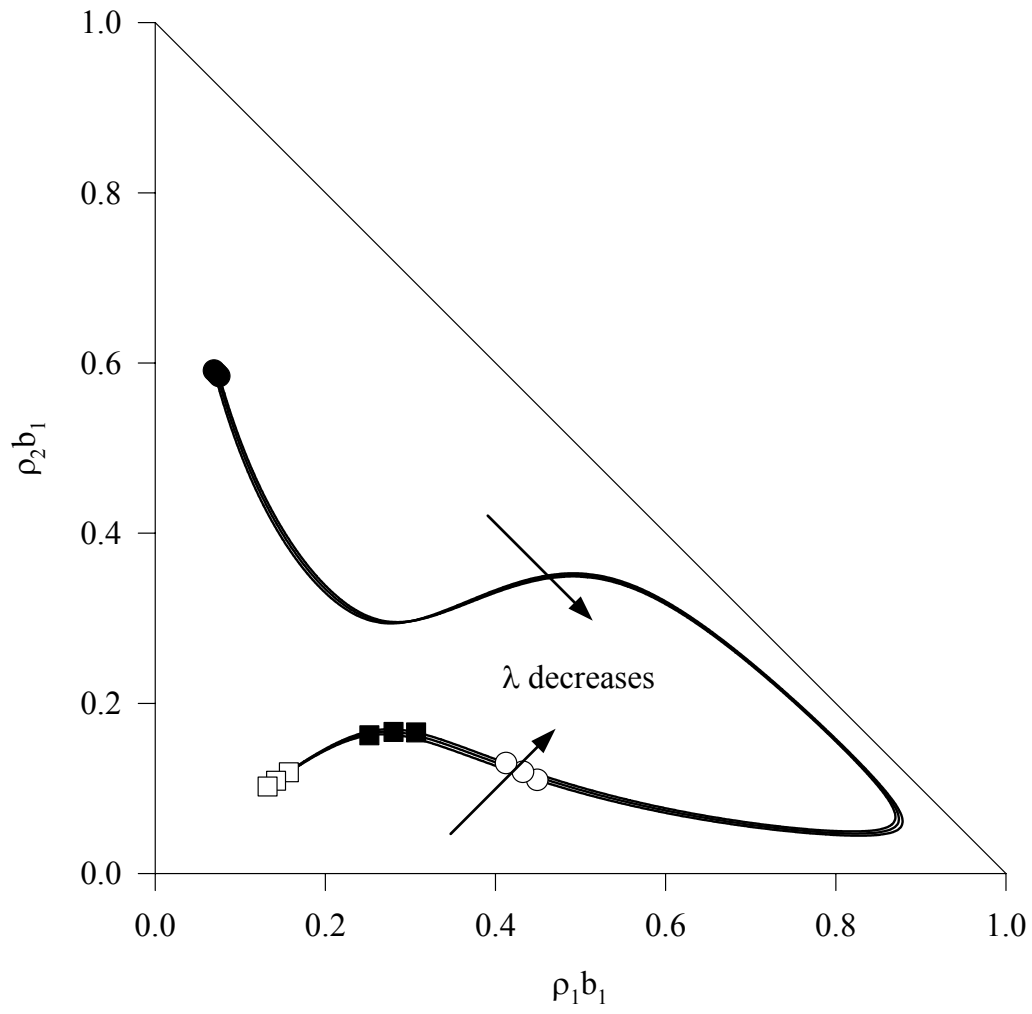


Figure 7

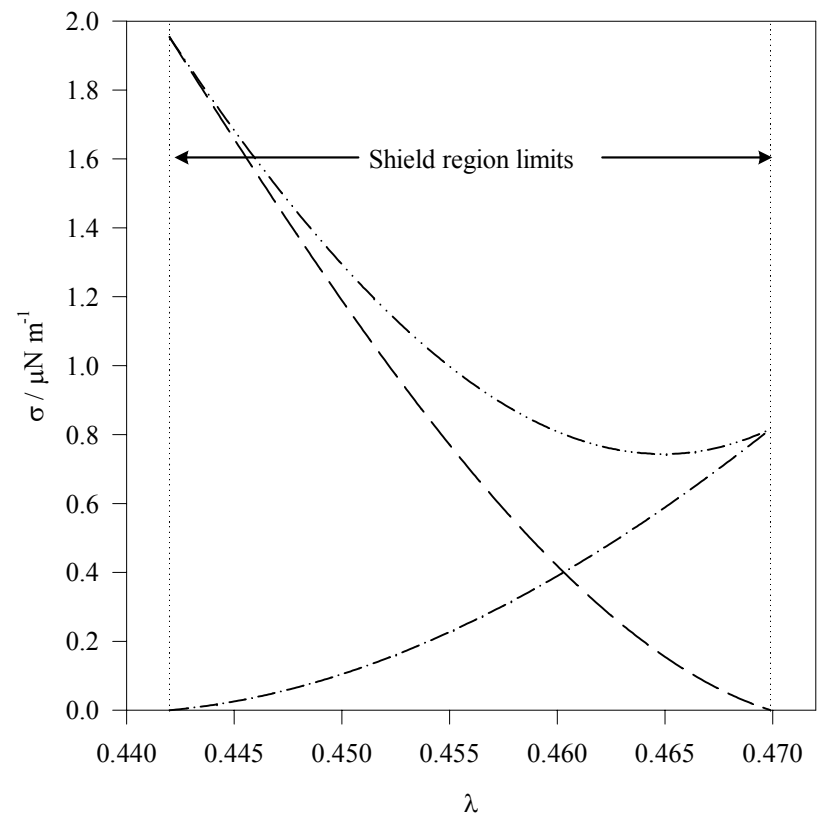
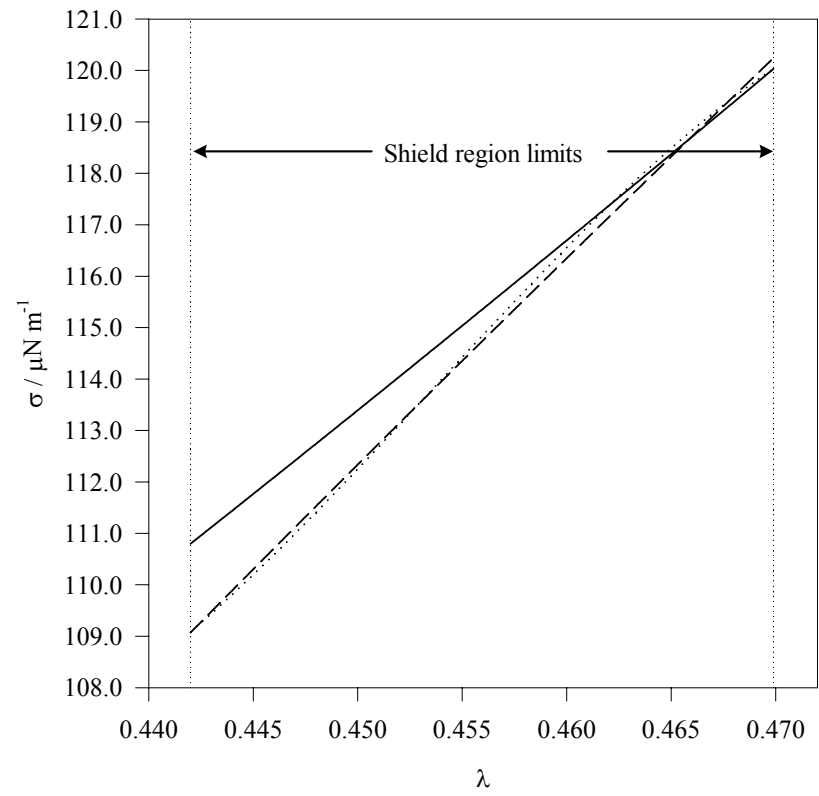


Figure 8

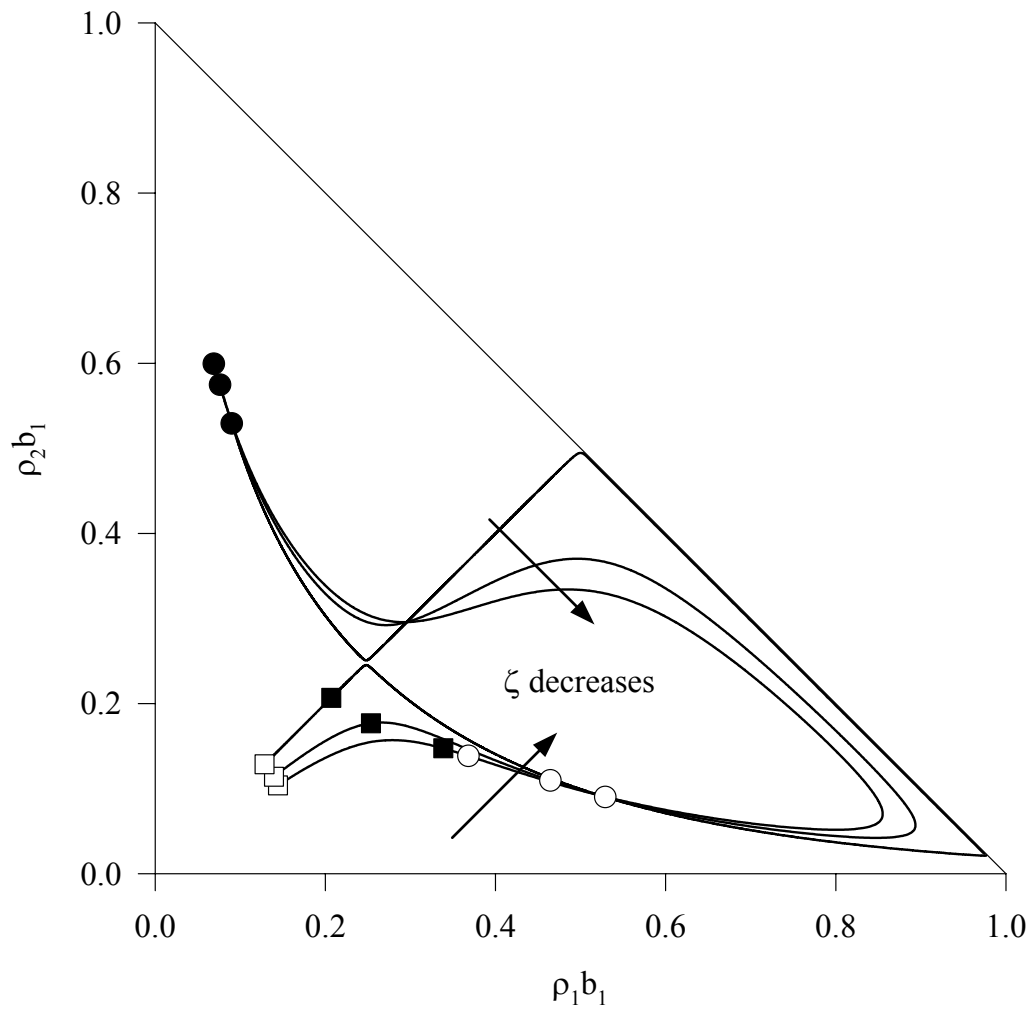


Figure 9

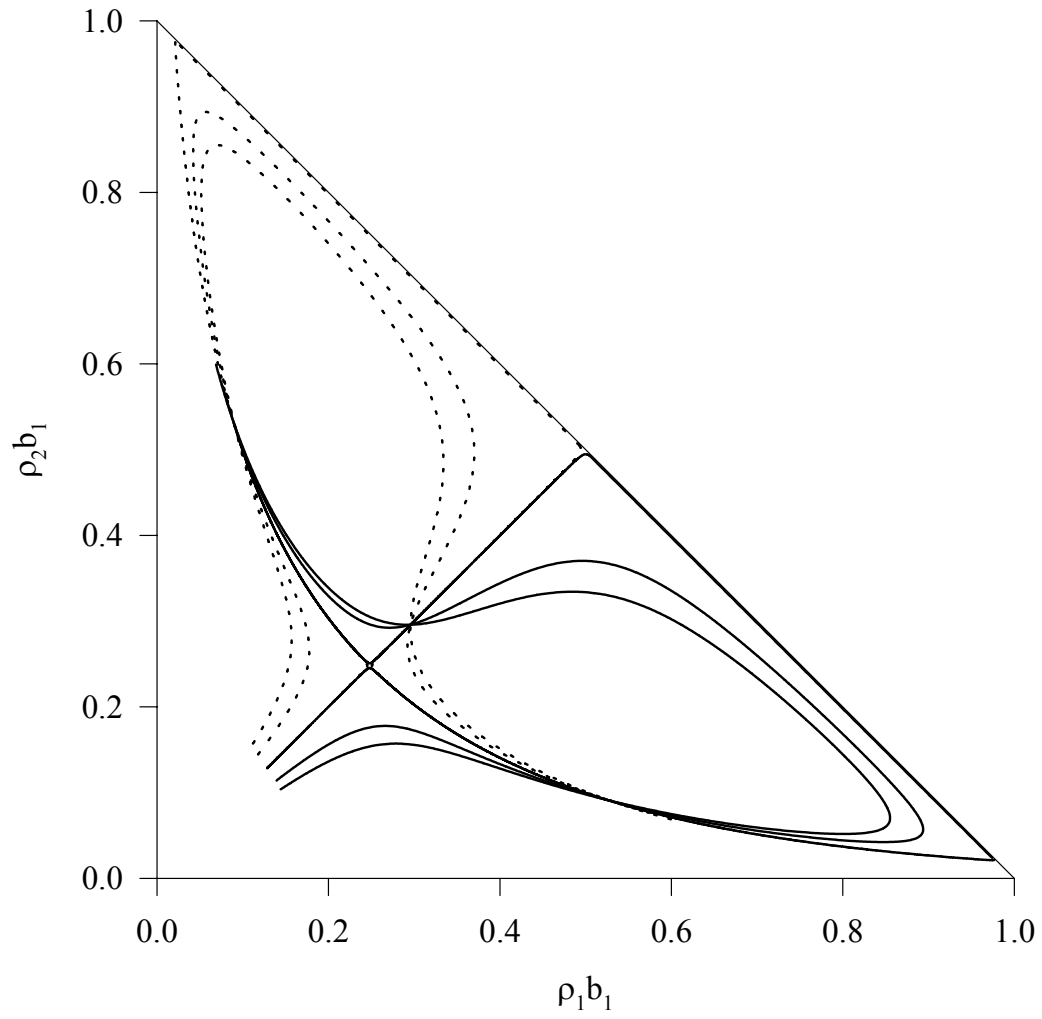


Figure 10

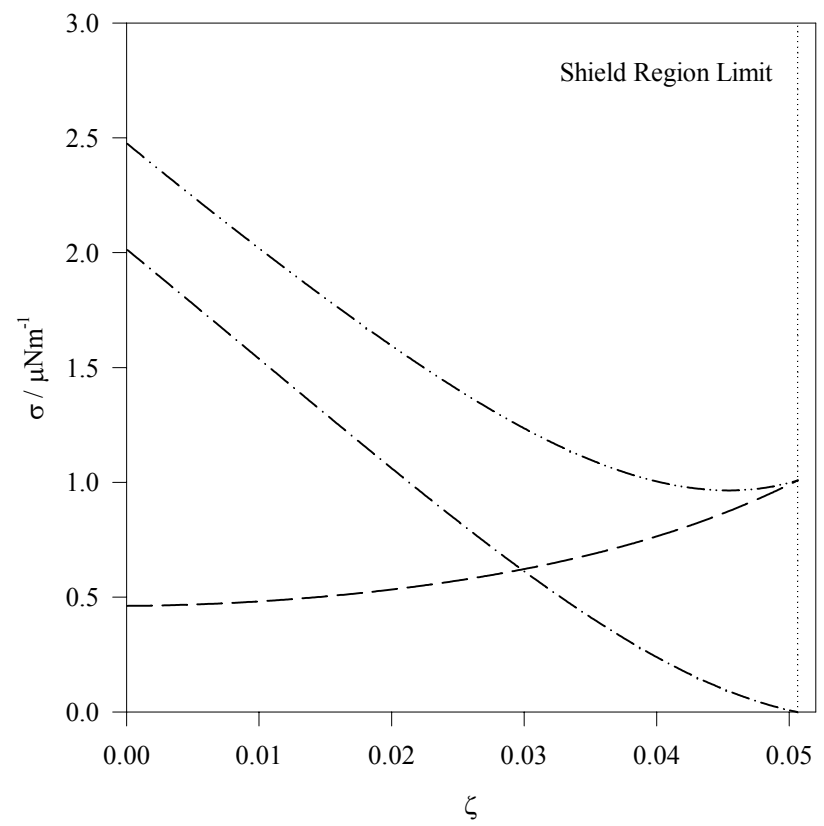
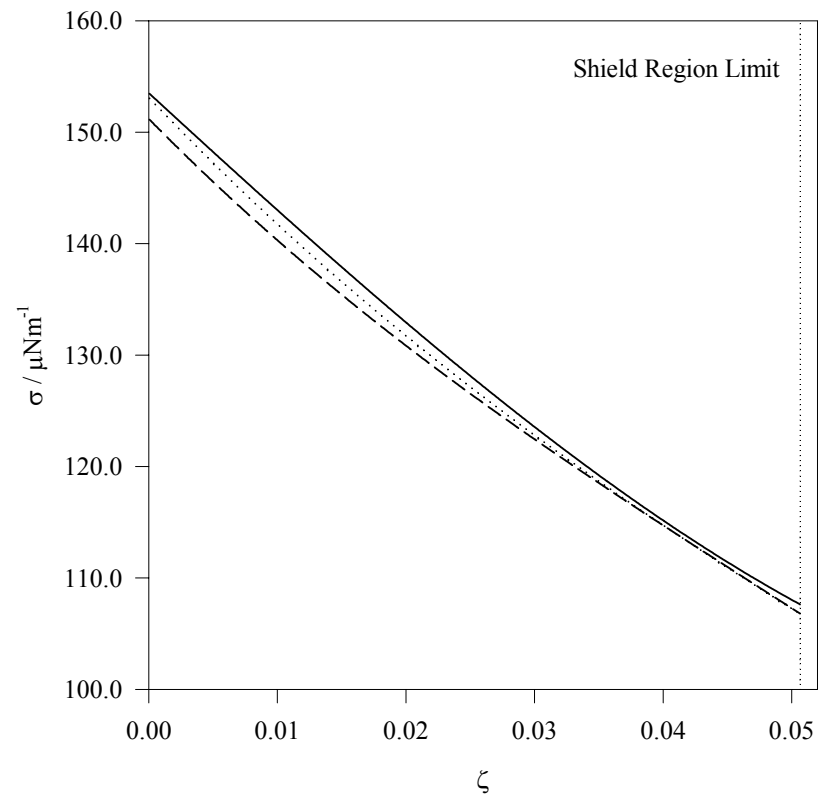


Figure 11